CrossMark

ORIGINAL ARTICLE

Morphological, structural, and functional alterations of the prefrontal cortex and the basolateral amygdala after early lesion of the rat mediodorsal thalamus

Zakaria Ouhaz[1] · Saadia Ba-M'hamed[1] · Mohamed Bennis[1]

Abstract Early postnatal damage to the mediodorsal thalamus (MD) produces deficits in cognition and behavior believed to be associated with early prefrontal cortical maldevelopment. We assessed the role of MD afferents during development on the morphological and functional maturation of the prefrontal cortex (PFC) and the basolateral amygdala (BLA). Sprague—Dawley rat pups ($n = 56$) received a bilateral electrolytic lesion of the MD or a MD Sham lesion on postnatal day 4. 7 weeks later, all rats were tested in anxiety-related and cognitive paradigms using the elevated plus maze and novel object recognition tests. Following behavioral testing (P70), rats were killed and the baseline expression of C-Fos protein and the number of GABAergic neurons were evaluated in the PFC and the BLA. The dendritic morphology and spine density in the PFC using Golgi-Cox staining was also evaluated. Adult rats with early postnatal bilateral MD damage exhibited disrupted recognition memory and increased anxiety-like behaviors. The lesion also caused a significant diminution of C-Fos immunolabeling and an increase of the number of GABAergic neurons in the PFC. In the BLA, the number of GABAergic neurons was significantly reduced, associated with an increase in C-Fos immunolabeling. Furthermore, in the PFC the lesion induced a significant reduction in dendritic branching and spine density. Our data are consistent with the hypothesis that the MD plays a role in the development of the PFC and, therefore, may be a good animal model to investigate cognitive symptoms associated with schizophrenia.

Introduction

The prefrontal cortex (PFC) originally defined as the projection area of the mediodorsal thalamus (MD; Rose and Woolsey 1948) was confirmed by further anatomical studies in both rodents (Guldin et al. 1981; Groenewegen 1988; Uylings et al. 2003) and primates (Goldman-Rakic and Porrino 1985; Giguere and Goldman-Rakic 1988). However, the functional significance of the MD-PFC circuitry has remained somewhat elusive, specifically with regard to the impact of developmental changes in the MD on the development and function of the prefrontal cortex and related brain areas such as the amygdala.

It is widely accepted that cortical development is experience- and activity-dependent (Van Ooyen et al. 1995; Rajan and Cline 1998). Using tract-tracing techniques, early studies in rodents have shown that MD fibers arrive in the PFC, mainly in layer III, at birth and increase in density through P10 (Leonard 1969; Krettek and Price 1977; Van Eden 1986). By P4 and P5, layer V can be distinguished from the upper cortical plate. However, myelination of axons, a marker of mature axons, from the MD to the PFC is completed approximately in the second decade of life (Benes 1989). Notably, changes in the quantity of MD fibers appear to mirror and precede volumetric alterations in the PFC, further suggesting that the MD plays a critical regulatory role in prefrontal cortical development (Van Eden and Uylings 1985; Van Eden 1986; Rios and Villalobos 2004).

✉ Mohamed Bennis
  mbennis@uca.ac.ma

[1] Lab of Pharmacology, Neurobiology and Behavior (URAC-37), Faculty of Sciences Semlalia, Cadi Ayyad University, 40000 Marrakech, Morocco

Springer

The infralimbic and prelimbic subregions of the PFC are connected with the rostral thalamus, the MD, the medial geniculate nucleus and basolateral nucleus of the amygdala (BLA; Krettek and Price 1977; Ottersen and Ben-Ari 1979; Su and Bentivoglio 1990). Despite the belief that the PFC regulates amygdala outputs and the accompanying behavioral phenomena (Bishop et al. 2004; Quirk and Beer 2006), little is known about the postnatal development of PFC–BLA connectivity. Several studies have shown that the amygdala is robustly connected with the mPFC in rats (Sesack et al. 1989; Hurley et al. 1991; McDonald 1991; Berendse et al. 1992; McDonald et al. 1996; Vertes 2004) and in non-human primates (Room et al. 1985; Chiba et al. 2001; Ghashghaei and Barbas 2002). These studies concur that the dorsolateral (DL), prelimbic cortices (PrL), and the BLA are reciprocally connected (Cassell et al. 1989; Hurley et al. 1991; Berendse et al. 1992; Shinonaga et al. 1994; McDonald et al. 1996; Sah et al. 2003).

Accordingly, disturbances localized at one of the three nodes (MD, PFC, and BLA) along this pathway have been demonstrated to be a key feature of different psychiatric disorders of potential developmental origin such as schizophrenia (Broadbelt et al. 2002; Volk and Lewis 2003; Phelps and LeDoux 2005). The MD has further become a focus of attention in the study of the pathological processes underlying the onset of a number of neuropsychiatric symptoms. Behavioral studies in monkeys or rodents have indicated that the MD is involved in learning, memory, decision-making, fear conditioning, anxiety, and impaired social interactions.

(Isseroff et al. 1982; Floresco et al. 1999; Chauveau et al. 2005; Parnaudeau et al. 2013, 2015; Ouhaz et al. 2015). Recent research has challenged the dogma of MD role as a passive nucleus and has identified a protracted critical period when this nucleus is in a position to exert a critical regulatory role over plasticity and maturation in the PFC (Marmolejo et al. 2012).

Recently, we have studied the long-term cognitive and behavioral effects of early developmental insult to the MD in adult rats. Rats that received an early MD lesion at postnatal day 4 display in adulthood a variety of abnormalities in a number of behaviors (Ouhaz et al. 2015), which bear close resemblance to behaviors seen in animals sensitized to psycho-stimulants (Lipska and Weinberger 1993; Maaswinkel et al. 1996) including high levels of anxiety, impaired social behavior, learning and working memory problems, and stereotypic behaviors (Ouhaz et al. 2015). Many of the cognitive and behavioral features showed parallels to schizophrenia-like symptoms.

Among the numerous neural and cellular alterations that have been proposed to underlie aspects of schizophrenia symptomology, several reports have identified decreased dendritic arbor and spine density of prefrontal cortical pyramidal neurons in postmortem schizophrenic brains (Garey et al. 1998; Glantz and Lewis 2000; Broadbelt et al. 2002; Volk and Lewis 2003). Other reports suggest that prefrontal GABA transmission may be a key contributor to cognitive impairment associated with the disease. Alterations in the expression of markers of GABA function are amongst the most highly reproducible pathologies observed in postmortem schizophrenic brains (Akbarian et al. 1995; Volk et al. 2000; Thompson et al. 2009). Optimal prefrontal GABA transmission is thought to be critical for generating neural oscillations, particularly in the gamma range, that underlie cognitive functions such as working memory (Howard et al. 2003; Gonzales-Burgos and; Lewis 2008).

Based on these findings, we evaluated the role played by MD afferents on the morphological organization and the function of the PFC and the BLA. We hypothesized long-term altered morphology, neuronal activation, and disrupted GABAergic neurotransmission in both structures as a consequence of early MD damage. We also hypothesized that, if the influence of the MD is critical for the normal, ongoing development of the PFC from the earliest postnatal stages of brain maturation, then surgical lesions of the MD induced just after birth should cause long-term alterations in the morphology and the activity of both the PFC and BLA in adult rats. Therefore, the present study tested these widespread changes using (1) the elevated plus maze and the novel object recognition tests to assess anxiety-related behavior and cognitive changes, (2) the modified Golgi-Cox staining procedure to quantitatively evaluate the dendritic development in the PFC, and (3) immunohistochemical procedures to examine neuronal activation (using C-Fos expression) and changes in the number of GABAergic interneurons in both the PFC and BLA.

Materials and methods

In a previous investigation, we showed that MD lesions performed at P4 in rats result in behavioral and cognitive changes related to the disruption of the PFC–MD communication and that this disturbance altered the development of the PFC (Ouhaz et al. 2015). In the present follow-up study, we assessed the anatomical and functional alterations following early MD lesions during the same critical period of brain maturation. The present experiments used 56 Sprague–Dawley male rats bred in the central animal care facilities of Cadi Ayyad University, Marrakech, Morocco. Pregnant rats were individually housed in a temperature- and humidity-controlled environment on a 12 h light/ dark cycle with free access to food and water. All animal procedures were in strict accordance with guidelines of the European Council Directive (EU2010/63). All efforts were made to minimize any animal suffering, and the study met

the ethical standards and approvals of the Council Committee of the research laboratories of the Faculty of Sciences, Cadi Ayyad University of Marrakech.

Surgery

Date of birth was defined as the first postnatal day (P0). On postnatal day P4, pups (weighing 7–8 g) were anesthetized by hypothermia for 6 min and positioned in an adapted platform fixed to a stereotaxic apparatus (David Koff instrument) using aseptic conditions. Animals were randomized into two groups: MD lesion group and MD sham group (n = 28 per group). The scalp of all animals was retracted and the skull was gently exposed over Bregma and the intended lesion site. For the MD lesion, stereotaxic coordinates were determined in a preliminary study using the atlas of Paxinos and Watson (2008).

Because the skull had not yet ossified, scissors were used to cut an opening for the electrode to penetrate through the brain using the following coordinates from Bregma: AP = 1 mm caudal to Bregma, $L = \pm 0.5$ mm lateral to the midline and $P = 3.5$ mm deep from dura on each side. In the MD lesion group, a current of 5 mA (tip negative) was passed for 7 s. In the MD sham group, the electrode was descended and removed without passing current. The wound was re-sealed using superglue (Aradine, Morocco). After the procedure, the wounds were cleaned with Betadine 10% (Pharma Laboratory, Morocco), and the pups were placed on a heated pad for recovery and subsequently returned to their mothers, where they stayed until weaning at postnatal day P30. During the post weaning period, groups of 5 animals were formed and housed in cages of (34 × 24 × 18 cm). 7 weeks post-surgery (P53), rats were trained in the behavioral paradigms to assess anxiety and cognition. Body and brain weights were measured at P70, after which all animals were sacrificed at P70 and the brains collected for either histological staining, Golgi-Cox staining, or immunohistochemistry.

Behavioral testing

Prior to behavioral testing, all animals were gently handled for 2 min/day during 1 week prior to the start of training. In addition, they were individually familiarized with the testing room and the test arena for 5 min/day during the daily handling prior to training.

Behavioral testing was conducted during sessions between 9 AM to 12 AM. All animals (n = 56) from the two groups were tested (n = 5 or 6 per session), and behavior recorded and analyzed using Ethovision XT Noldus 8.5 video-tracking program (*Noldus Information Technology b.v., Wageningen, The Netherlands*). The video camera (JVC) was positioned 2.5 m above the arena so as to cover the entire view of the arena. Two tracking points were specified: one the head and the other the center of gravity of the animal. After testing each rat, any debris was removed from the maze, and all interior surfaces, walls, and floors were cleaned thoroughly with 70% ethanol, followed by water, and then wiped dry. At least 5 min was allowed between testing each individual animal to ensure the maze was completely dry and any residual odor of alcohol had dispersed before the next rat was introduced into the maze.

Elevated plus maze test

The elevated plus maze is a widely accepted paradigm used to assess anxiety-like behavior in rodents (Handley and McBlane 1993; Handley and Mithani 1984; Lapiz-Bluhm et al. 2008). The elevated plus maze (plexiglass) had two opposing open arms (50 × 5 cm) and two closed arms (50 × 5 × 15 cm) connected through a square central area (5 × 5 cm). The entire apparatus was elevated to a height of 45 cm above the floor. For testing, the rat was removed gently from its home cage and placed in the central arena of the elevated plus maze facing the junction of an open and closed arm. The experimenter retired behind a screen to be shielded from the rats' view. The rat was allowed to freely explore the maze for 5 min, while their behavior was recorded for offline analysis. The time spent in the open arm over the total time spent on both arms and the number of entries to the open arm vs the total number of entries was quantified during the test session.

Novel object recognition test

The apparatus consisted of an open field (100 × 100 × 50 cm high) made of Plexiglas with the inside painted matt black. The objects to be discriminated were available in three copies and made of plastic. We employed the protocol described by Ennaceur and Aggleton (1994) for a one trial non-matching to sample learning procedure. The 'identical' to-be-familiarized (sample) objects (approximately 10 cm) was placed in the back left and right corners of the apparatus, and before starting the video tracking, a card with the animal's identification number was placed within the recording field. The animal was positioned at the midpoint of the wall opposite the sample objects. When placed into the maze, the animal was placed with its body parallel to the side walls and nose pointed away from the objects to prevent any unintentional bias in placement. After the sample-object exposure time (10 min), the animal was removed from the apparatus and returned to its home cage for the training-to-testing interval (60 min). To test recognition after this interval, one familiar sample object and the novel object were placed in the middle of the back wall. Finally, the animal was positioned in the apparatus as described

above, and the testing session lasted for 5 min. The animal was then removed and returned to the home cage. Time with familiar object vs novel object and discrimination ratio (novel object interaction/total interaction with both objects) were scored.

Golgi-Cox staining

After the behavioral testing (at P70), 28 rats (MD lesion = 14 and MD sham = 14) were deeply anesthetized with urethane (40 mg/kg) and sacrificed by decapitation. The brains were removed and the anterior part was processed for Golgi preparation as described by Armstrong and Parker (1986). Specimens were processed in pairs. Tissue from MD sham and MD lesion rats was cut into 2 mm slabs and wrapped in gauze. The tissue was first placed in a solution containing 100 ml H₂O, 3 g potassium dichromate, 12.5 g sucrose, 5 ml Formol (37%), and 7.5 ml of 3% H_2O_2 and incubated in an oven at 55 °C for 6–7 h. The tissue was removed from the oven and placed in a fresh solution and left at room temperature overnight. The following day, the tissue was placed in a second solution containing 100 ml d'H₂O, 3 g potassium dichromate, and 12.5 g sucrose, and incubated in an oven at 55 °C for 6–7 h. The tissue was then removed and left at room temperature overnight in a fresh solution. On the following day, the tissue was rinsed in 0.75% silver nitrate and placed in fresh 0.75% silver nitrate for 5 days at room temperature. Finally, the tissue was serially sectioned on a vibratome (Leica VT 1200 S) into 50-μm thick sections and collected in 70% ethanol. The sections were dehydrated in graded ethanol starting from 70%, defatted in xylene, and mounted onto gelatin-coated slides and coverslipped.

Identification of regions of interest: The slides containing the medial prelimbic (PrL), dorsolateral anterior (DL) and cingulate (Cg1) areas were determined according to the atlas of Paxinos and Watson (2008). All of the sections containing the PFC regions were analyzed for dendritic morphology.

Quantification of the Golgi material

Pyramidal neurons impregnated with Golgi-Cox solution were identified by their characteristic triangular soma shape, apical dendrites extending toward the pial surface, and numerous dendritic spines. The criteria used to select neurons for reconstruction were those described by Silva-Gomez et al. (2003). Five neurons from each region of interest of each hemisphere per animal were drawn digitally. For quantitative analysis, single pyramidal neurons in layer V were fully reconstructed, dendritic spines included, viewed via a Nikon Eclipse 600 light microscope equipped with a motorized stage interfaced to the computer and

using Neurolucida 360 programs (*Microbrightfield Inc, VT*) at high magnification (100× oil immersion objective).

To evaluate the eventual morphological changes related to the early MD lesion, we quantified the following dependent measures: the maximum branch order which was estimated by the number of each dendritic bifurcation level over the total number of dendritic branches, expressed as a percentage, the total number of primary and secondary dendrites. The total number of spines over dendritic segments (primary and secondary dendrites) was obtained by the software program NeuroExplorer® 5.022 (*Microbrightfield Inc*) for all dendritic branches.

Sholl analysis

To assess the density of spines and the length of the dendritic field, Sholl analysis (Sholl 1953) was performed using Neurolucida and Neuroexplorer software. A randomly placed digital grid was overlaid on the region of interest and two points from the grid were selected randomly. The neurons closest to each selected point was chosen for analysis, subject only to the criterion that its apical dendrites continue for at least 100 μm within the section. For each neuron, the soma was traced first, followed by every single dendrite with its primary and secondary segments. Every spine emanating from the primary and secondary segments was traced. Dendritic processes were projected on a 2-dimensional model to allow quantitative analyses.

Immunohistochemistry

1 h after completing the behavioral testing, a cohort of 28 adult rats (P70; MD sham = 14 and MD lesion = 14) were deeply anesthetized with urethane 40% (1 g/kg, from Sigma–Aldrich, France), and then transcardically perfused with saline (0.9%), followed by 4% paraformaldehyde in phosphate-buffered saline (0.1 M). The brains were removed from the skull and postfixed in the same fixation solution for 12h, cryoprotected overnight in 30% sucrose, and then sectioned in the coronal plane at a 40 μm thickness using a cryostat (Leica Microsystems, Germany). All brains were processed together, and serial sections through the PFC and the amygdala were collected to be processed for immunohistochemical staining using antibodies directed against C-Fos protein and GABAergic neurons. At the beginning of the procedure, the slices were rinsed with PBS and then incubated with non-specific serum (0.1% Lysine, 0.5% Gelatin, and 0.3% Triton = PBS-L-G-T) for 60 min. For C-Fos immunostaining, an anti-C-Fos antiserum was used (Oncogene Research Products, Sandiego, Ab5, polyclonal rabbit pAb 1:500). For GABA immunostaining, an anti-GABA antiserum was used (Geffard,

Bordeaux, Polyclonal rabbit; 1:1000). The free-floating sections were incubated overnight at 4 °C with the primary antibodies diluted in PBS-L-G-T. Sections were rinsed four times (10 min each) in PBS Triton (PBS-T) and incubated for 3 h at room temperature in the secondary biotinylated goat anti-rabbit IgG (Vector Laboratories, Burlingame, CA, USA), diluted in 1:200 PBS-T. Sections were then rinsed in PBS, and incubated for 1 h 30 at room temperature in avidin-biotin-peroxidase complex (Vectastain Elite ABC Kit, Vector Laboratories, Burlingame, CA, USA; diluted in 1:200 PBS).

Finally, after rinsing four times in PBS-T, the peroxidase activity was visualized with 0.025% 3–3′-diaminobenzidine tetrahydrochloride in Tris buffer (Pre-set) 0.05 M, containing hydrogen peroxide (0.006%). Processing was stopped by rinsing sections for 4×10 min in PBS. Sections were mounted on gelatin-coated slides, dehydrated in graded series of ethanol, cleared in xylene and coverslipped with Eukitt.

Analysis of immunohistochemical data

Sections were obtained from each region of interest along its entire length; ten sections through PFC subregions and seven within the BLA of each animal. Regions of interest were identified according to the rat brain atlas of Paxinos and Watson (2008). The counting of C-Fos positive nuclei (a C-fos positive neuron (C-Fos+) refers to a neuron with a darkly stained nucleus) and /or GABA positive cell bodies (GABA+ neuron refers to a neuron with dark soma and dark edges) was performed bilaterally and blindly by the same observer using ImageJ ® software. The threshold criterion for positive immunostaining was set at the level that selected the darker stained nuclei/cell bodies, without selecting the background staining. The setting for illumination was kept constant through the analysis.

Analysis of the total number of positive stained cells was determined using Abercrombie's formula for stereological analysis (Abercrombie and Johnson 1946): $p = (1/f)\ AM/(D+M)$, where p is the total number of positive stained cells in the nucleus, f is the frequency of the selected sections used for immunostaining, A is the gross cell count, M is the thickness of the sections (μm), and D is the average diameter of cell nuclei (μm). The same counting procedures were applied to all groups.

Stereological evaluation of the lesion

The caudal portions of the brain used for both Golgi-Cox impregnation and immunohistochemistry were kept for the verification of the lesion. Coronal sections of 40 μm were obtained at the level of MD on gelatin-coated slides. Sections were stained with 0.1% Cresyl violet and examined under a light microscope (Olympus BH-2) equipped with a camera (Olympus DP.71).

Data analysis

Statistical analysis was performed using SigmaPlot 11.0 software. Two groups' comparisons were performed using Student's t test or the non-parametric Mann–Whitney U test. The main effect of each independent variable was assessed using the two-way ANOVA procedure, followed by post hoc testing with the Holm-Sidak method for pairwise multiple comparisons. All tests were two-tailed and the significance threshold was set at $p < 0.05$.

Results

MD thalamic lesion

The evaluation of body weights (MD lesion: 267.28 ± 3.39 g; MD sham: 261.57 ± 5.30 g; $t(ddl = 54) = 0.32$; $p > 0.05$) and brain (MD lesion: 2.04 ± 0.040 g; MD sham: 2.06 ± 0.035 g; $t ddl = 54) = 0.31$; $p > 0.05$) revealed no lesion effect on both dependent variables. The electrolytic lesion of the mediodorsal thalamic nucleus (MD) performed at P4 induced an extensive damage within this structure in all adult experimental rats (Fig. 1). The lesion site showed a considerable loss of neurons, leading to a significant decrease of the total volume of the nucleus, and spreading to its most lateral portions. The lesion caused only a limited damage to the habenulae and to the thalamic paraventricular nucleus (Fig. 1a, b).

Behavioral testing

Elevated plus maze test

Animals' exploration of the maze (Fig. 2a–d) was assessed by comparing the total number of entries. The statistical analysis using Student's t-test failed to demonstrate any significant difference in exploratory behavior between the two groups (MD sham and MD lesion) [$t(ddl = 54) = 0.43$, $p > 0.05$] (Fig. 2a). However, the MD lesion rats visited the open arms less frequently compared to the MD sham rats (Fig. 2b). Student's t test confirmed that this difference in the mean number of open arms entries was significant, [$t(ddl = 54) = 12.15$, $p < 0.001$]. In addition, the MD lesion group spent less time in the open arms, the ratio was (0.1 ± 0.08) compared to the MD sham (Fig. 2c, d). Student's t test confirmed that this difference in exploration times was significant [$t(ddl = 54) = 11.37$, $p < 0.001$].
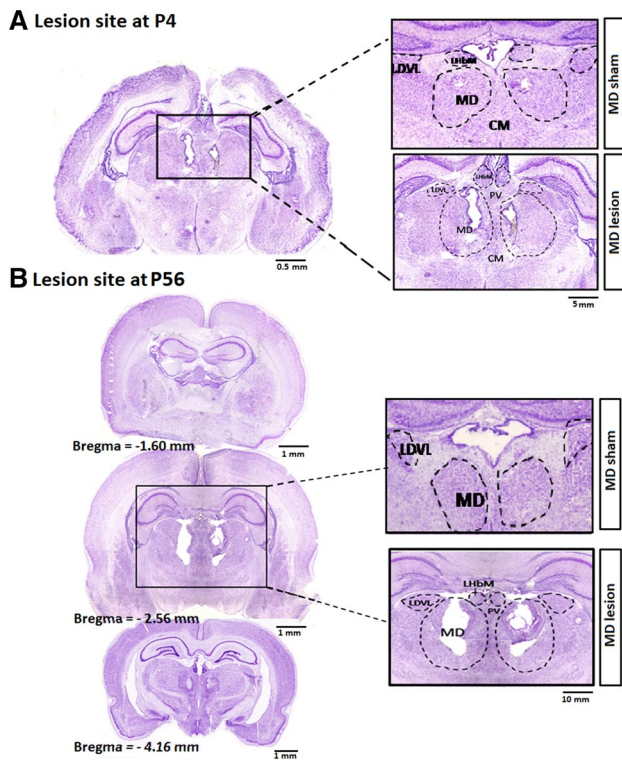
Fig. 1 **a** Photomicrograph detailing the lesion site in MD lesion and MD sham rats at P4. **b** Consecutive photomicrographs of brain sections before, and after the lesion site of MD lesion and MD sham adult rats. *Numbers* represent the distance from Bregma

The novel object recognition test

The assessment of object recognition was reflected by greater time interacting with the novel than the familiar object, and a discrimination ratio above 0.5 (Fig. 2e–h). During the testing session, total locomotor activity showed no statistical differences among the experimental groups [t(ddl = 54) = 0.63, $p > 0.05$] (Fig. 2e). Nonetheless, the total time spent in interaction with both objects has significantly decreased following the early MD lesion [t(ddl = 54) = 41.08, $p < 0.001$]. Furthermore, MD lesion rats spent less time exploring the novel object compared to MD sham rats (Fig. 2f, h). The two-way ANOVA test (with the lesion condition and the object nature as main factors) confirmed these differences; the lesion [F(2.83) = 201.668, $p < 0.001$] and the object nature [F(1.83) = 193.10, $p < 0.001$] had significant effects on interacting time and the interaction between the two factors was also significant [F(2.83) = 354.16, $p < 0.001$]. *Post hoc* analysis showed that the MD lesion group spent significantly more time exploring the familiar object compared to the novel one (t = 13.67, $p < 0.001$), whereas the MD sham animals spent longer time interacting with the novel object (t = 17.86, $p < 0.001$). The discrimination ratio, expressed as the

novel object interaction frequency over total interaction with objects, revealed that the MD lesion group interacted less with the novel object compared to MD sham groups (Fig. 2g). The Kruskal–Wallis one-way ANOVA test confirmed these differences [H(ddl = 1) = 28.22, $p < 0.01$].

Quantification of the Golgi-Cox material

Dendritic morphology

The morphological analysis presented in this study was based on a total of 504 neurons from 24 animals. Branching complexity of apical and basal dendrites, and dendritic length and spine densities were quantified in 168 neurons from the DL (MD sham = MD lesion = 84), 168 neurons from the PrL (MD sham = MD lesion = 84), and 168 neurons from the anterior Cg1 (MD sham = 88; MD lesion = 80; Fig. 3a). Thus the dendritic morphology was analyzed for each of the lesion conditions and in the main subregions of the prefrontal cortex that receive afferents from the MD.

The spatial organization of dendritic arbors was estimated by evaluating the maximum branch order levels. The critical measurement reflected the percentage of each branching level over the total number of dendritic branches (branching, indicated by bifurcation), which was counted at each order away from the cell body or dendritic shaft (Fig. 3b). The dendrites emerging from the cell soma were considered as the first level, their first branches were second level of branching and so on, with increasing order until the tips were reached. This method quantifies the branching pattern of a neuron and the spatial degree of arborization, two important factors to determine the potential for connectivity.

Dendritic branch order. In all PFC subregions, pyramidal neurons of MD sham rats exhibited a normal morphological aspect of their dendritic tree, the highest level of branching was the 7th order and the maximum of branching order was the 4th level (Table 1; Fig. 3c–f). In contrast, the density of dendritic arborization of neurons from the MD lesion group was reduced, the highest-level of branching was the 3rd order and the maximum branching order was the 2nd (Table 1; Fig. 3c–f). Statistical analysis using two-way ANOVA (with the lesion condition and the branching level as main factors) revealed that the early MD lesion caused a significant reduction of the dendritic arbor by decreasing its maximum level of branch orders (Table 1).

Primary dendrites. Primary dendrites emerge directly from the cell soma, while their branches constitute the secondary dendrites. The morphology of stained pyramidal neurons from layer V showed a decrease in the total number of primary dendrites in pyramidal neurons from the MD lesion group (Fig. 4a, b). The two-way ANOVA
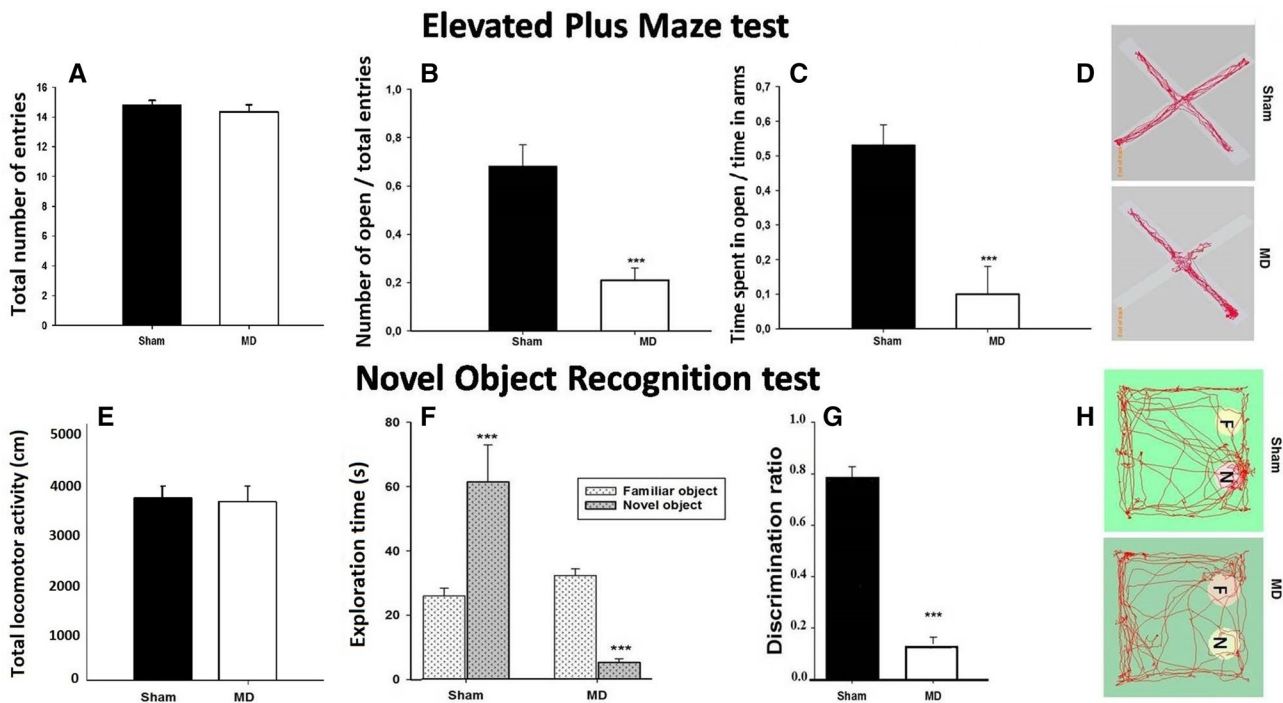
Fig. 2 Behavioral changes in adult rats caused by MD lesion at postnatal day 4 (P4). **a–d** Assessment of anxiety in the elevated plus maze test: **a** Total number of entries. **b** Mean ratio (R) number of entries in *open arms* over the total entries made into each area. **c** Mean ratio (R) between the times spent in the *open arms* relative to the time spent in the *open arms*. **d** Example of automated path tracking (*red curved lines*) of two experimental rats after task obtained using Ethovision video-tracking software (Noldus). **e–h** Novel object recogni-tion test using the non-matching-to-sample task. **e** Total locomotor activity (cm). **f** Mean of exploration time of the novel object vs the familiar object. **g** Mean of discrimination ratio. **h** Example of auto-mated path tracking (*red curved lines*) of two experimental rats in the task obtained using Ethovision video-tracking software (Noldus), **f** familiar object, **n** novel object. Data presented as mean $\pm$ SEM, ***p < 0.001 refers to the comparison between the MD sham vs MD lesion groups

method, considering the lesion conditions and the PFC subregions as main dependent factors, confirmed the significant effect of the early MD lesion on the development of pyramidal neurons' primary dendrites (Table 2).

Secondary dendrites. Morphological analysis also revealed that the early MD lesion produced a significant reduction of the total number of secondary dendrites in the three PFC subregions (Fig. 4c). The two-way ANOVA (lesion and the region of interest as main factors) demonstrated that the lesion decreased significantly the total number of secondary dendrites of layer V pyramidal neurons in comparison to MD sham animals (Table 2).

Dendritic spine density

Spine density along primary dendrites. The two-way ANOVA (lesion and PFC subregion as main factors) clearly showed a significant effect of the early MD lesion on the spine density along the primary dendrites (Fig. 5a, b; Table 3).

Spine density along secondary dendrites. Morphological analysis of layer V neurons of the PFC demonstrated that

the early MD lesion resulted in a reduced the spine density in secondary dendrites at P70 (Fig. 5c). The two-way ANOVA analysis (lesion and PFC subregion as main factors) confirmed that the differences between the MD lesion group and the MD sham were significant (Table 3).

The Sholl analysis

To better understand alterations in the spine density after an early MD lesion performed at P4, we examined the density of spines vs the distance from the soma. Using Sholl analysis, somata with radiating primary and secondary apical dendrites were traced in layer V pyramidal neurons of the three PFC subregions (Fig. 6a). In each PFC subregion, the pooled Sholl curve of the stained neurons of MD lesion animals was located markedly below the Sholl curve of those from the MD sham group at each distance from the soma studied. The proximal dendritic segments were defined as the segments with the radius of the concentric shell intersecting the dendritic tree at 20 μm distance from the soma, and for the distal segment (radius = 60 μm). Dendritic segments analyzed
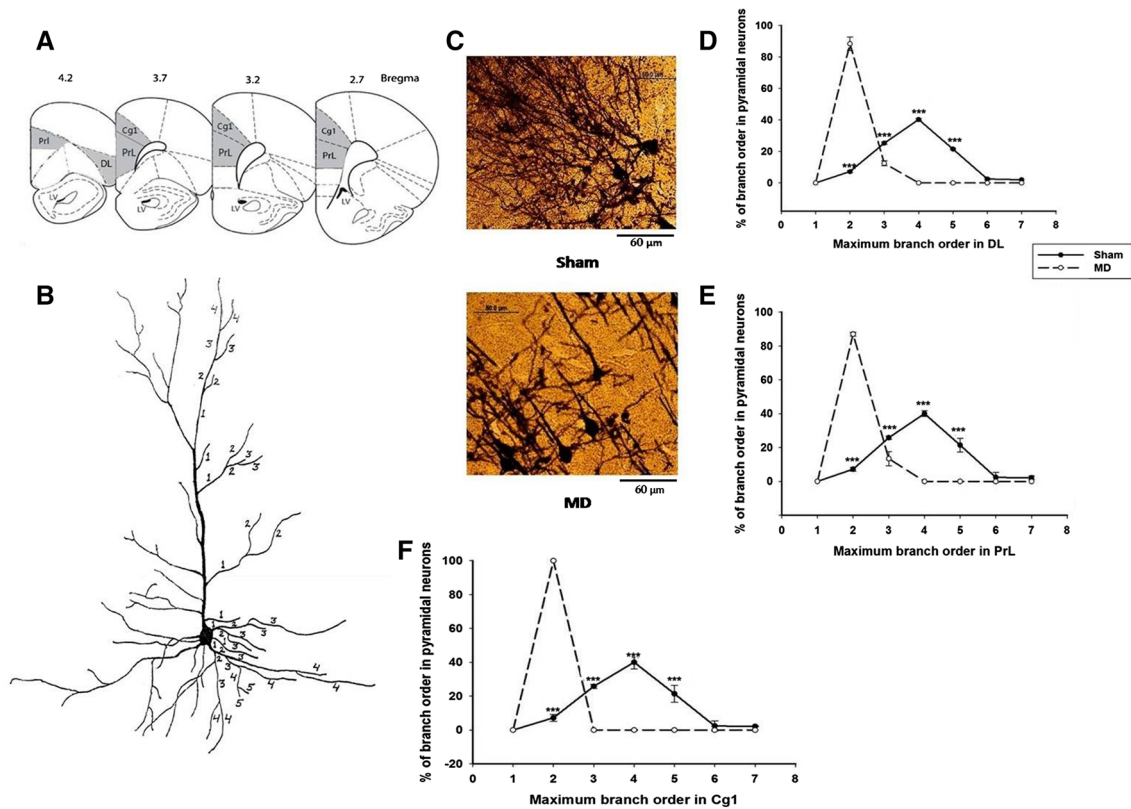
Fig. 3 Changes in branch orders of pyramidal neurons in the PFC of adult rats caused by MD lesion at postnatal day 4 (P4). **a** Schematic drawing of coronal rat brain sections of the PFC showing the three subregions of interest (in *gray*). **b** A schematic representation of a pyramidal neuron from the PFC layer V showing the branch centrifugal ordering. **c** Photomicrographs showing representative Golgi-Cox-impregnated pyramidal neurons of the PFC (PrL) from MD sham and MD lesion animals. **d** Mean percentage of branch ordering in the DL. **e** Mean percentage of branch ordering in the PrL. **f** Mean (±SD) percentages of branch ordering in the Cg1. Data presented as mean ± SEM ***$p < 0.001$ refers to the MD sham vs MD lesion groups' comparison. *DL* dorsolateral anterior cortex, *Cg1* cingulate area1 cortex, *PrL* prelimbic cortex

Table 1 Quantitative analysis of the maximum branch order by Two-way ANOVA comparison between MD sham and MD lesion animals followed by the *post hoc* analysis using Holm-Sidak (*t*) procedure
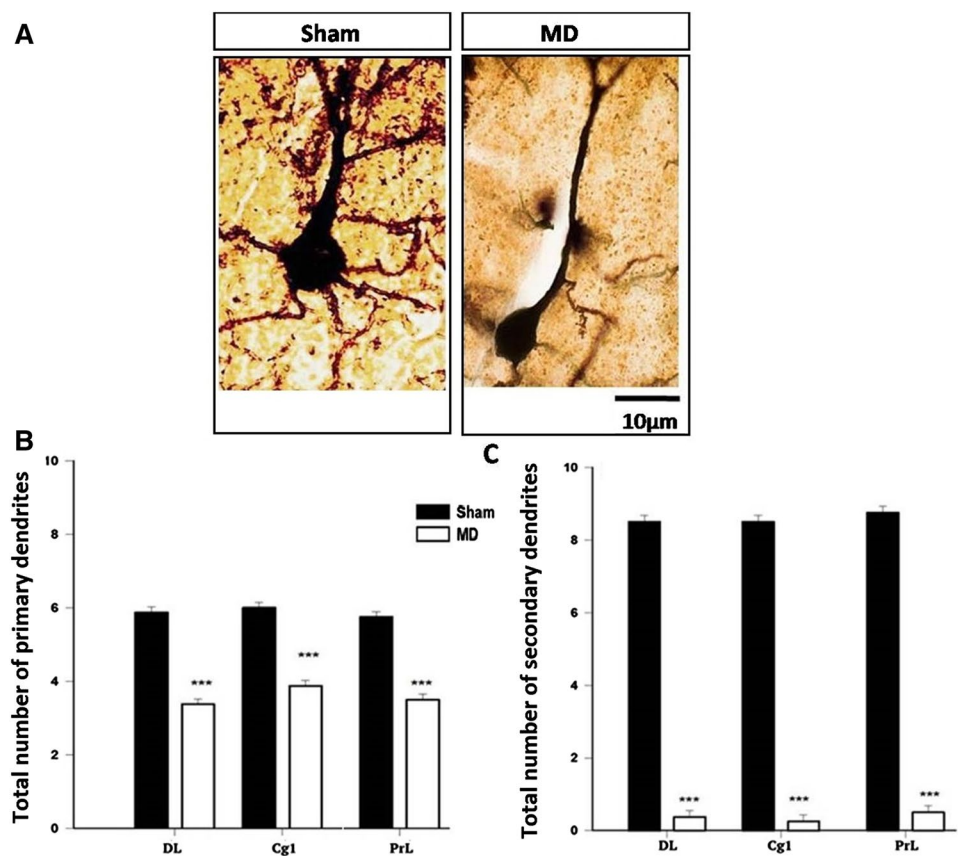
PFC subregions									
Branching Levels	DL			Cg1			PrL		
	MD sham (%)	MD lesion (%)	*t*	MD sham (%)	MD lesion (%)	*t*	MD sham (%)	MD lesion (%)	*t*
2nd	7.22 ± 0.79	88.43 ± 4.32***	13.11	7.21 ± 2.0	100***	28.39	7.21 ± 1.12	87 ± 1.17***	13.66
3rd	25.27 ± 0.73**	12.42 ± 1.60	3.09	25.82 ± 1.16***	0.00	6.57	25.82 ± 0.98*	13.42 ± 4.21	2.12
4th	40.30 ± 0.70***	0.00	6.60	40.04 ± 4***	0.00	13.25	40.04 ± 1.7 ***	0.00	6.90
5th	21.49 ± 0.49***	0.00	4.61	21.42 ± 5.02***	0.00	6.98	21.42 ± 4.12	0.00	1.22
6th	2.50 ± 0.60	0.00	0.04	2.36 ± 0.36	0.00	0.77	2.36 ± 0.94	0.00	0.40
7th	2.00 ± 0.00	0.00	0.32	2.14 ± 0.25	0.00	0.69	2.14 ± 1.07	0.00	0.36
Lc	$F(1.195) = 7.61**$			$F(1.195) = 12.8**$			$F(1.195) = 16.8**$		
Brl	$F(2.195) = 36.55***$			$F(2.195) = 33.22***$			$F(2.195) = 136.22***$		
Lc × Brl	$F(2.195) = 39.85***$			$F(2.195) = 40.10***$			$F(2.195) = 40.10***$		

DL dorsolateral anterior cortex, *Cg1* cingulate area1 cortex, *PrL* prelimbic cortex, *Lc* lesion condition, *Brl* Branching Level

*$p < 0.05$, **$p < 0.01$ and ***$p < 0.001$

Fig. 4 Changes in PFC basal and apical dendrites after early MD lesions. **a** Photomicrographs showing representative Golgi-Cox-impregnated pyramidal neurons of the PFC (PrL) from MD sham and MD lesion animals. **b** Mean total number of basal dendrites. **c** Mean total number of primary dendrites. **d** Mean total number of secondary dendrites. Data presented as mean ± SEM. ***$p < 0.001$

Table 2 Quantitative analysis of the percentage of primary and secondary dendrites loss by Two-way ANOVA comparison between MD sham and MD lesion animals followed by the *post hoc* analysis using Holm-Sidak procedure

Dendrites	PFC subregions	% of loss	Holm Sidak procedure	Lesion condition $F(1.47)$	PFC subregion $F(2.47)$	Lesion×subregion $F(2.47)$
Primary	DL	36.63	$t = 6.56$***	157.34***	0.66, ns	0.86, ns
	Cg1	37.50	$t = 6.79$***			
	PrL	46.25	$t = 8.37$***			
Secondary	DL	81.25	$t = 31.93$***	3122.56***	0.27, ns	0.08, ns
	Cg1	82.50	$t = 32.42$***			
	PrL	82.50	$t = 55.88$***			

*DL* dorsolateral anterior cortex, *Cg1* cingulate area1 cortex, *PrL* prelimbic cortex, *ns* non significant
***$p < 0.001$

at 20 μm in the DL (Fig. 6b) showed no significant decrease in spine density [$F(1.9) = 4.81$, $p = 0.06$], but at 60 μm, a significant decrease of 100% in spine density was observed [$F(1.9) = 4500$, $p < 0.001$]. In the Cg1 (Fig. 6c), the proximal segment showed no significant spine loss [$F(1.9) = 0$, $p = 1$], whereas in the distal segment a 100% was seen in MD lesion animals compared to MD sham controls [$F(1.9) = 48500$, $p < 0.001$]. In the PrL area (Fig. 6d), the one-way ANOVA showed a significant decrease of the spine density in the MD lesion group compared to the MD sham in both the proximal

[$F(1.9) = 3879.31$, $p < 0.001$] and the distal segments [$F(1.9) = 47531$, $p < 0.001$].

Evaluation of the dendritic length

The length of the dendritic arborization was determined by Sholl analysis using the procedure described above. Results confirmed that the early MD lesion affected the development and extension of dendrites by reducing the radial distance of pyramidal neurons. This morphological
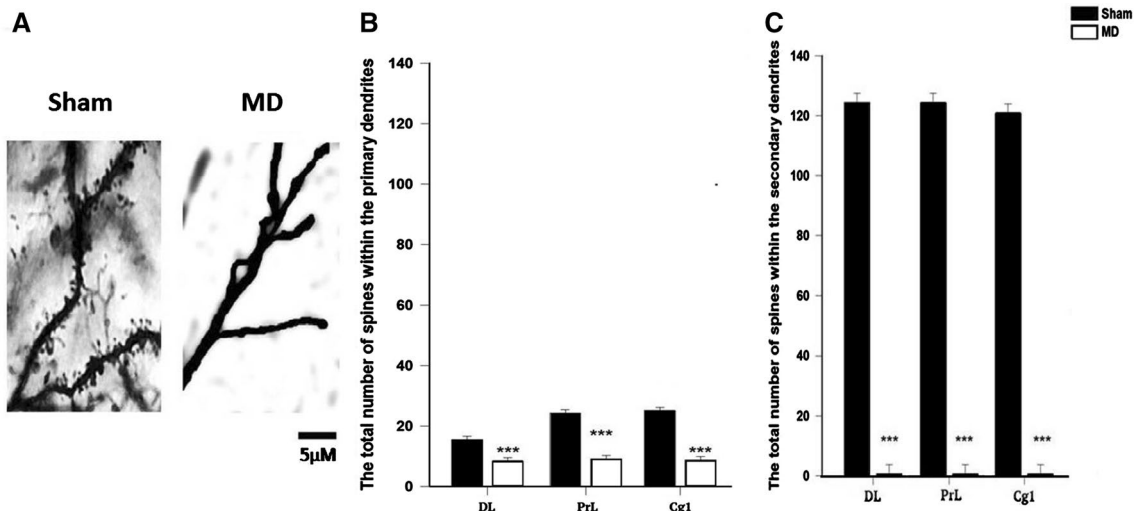
Fig. 5 Changes in total number of spines along apical dendrites. **a** Photomicrographs showing representative Golgi-Cox-impregnated spines of MD sham and MD lesion groups. **b** Mean total num-ber of spines within primary dendrites. **c** Mean total number of spines within secondary dendrites. Data presented as mean ± SEM. ***$p < 0.001$ refers to the sham vs MD lesion groups' comparison

Table 3 Quantitative analysis of spine number along primary and secondary dendrites by Two-way ANOVA comparison between MD sham and MD lesion animals, followed by the *post hoc* analysis using Holm-Sidak procedure

Spines along	PFC	MD sham	MD lesion	Holm Sidak procedure	Lesion condition $F(1.47)$	PFC subregion $F(2.47)$	Lesion × subregion $F(2.47)$
Primary dendrites	DL	22.75 ± 0.62	8.50 ± 0.59	$t = 16.70$***	1133.78***	10.76**	4.27**
	Cg1	28 ± 0.75	8.50 ± 0.50	$t = 22.08$***			
	PrL	25.75 ± 0.62	8.50 ± 0.59	$t = 19.53$***			
Secondary dendrites	DL	124.25 ± 6.13	0.5 ± 0.19	$t = 32.42$***	2142***	1.04, ns	0.08, ns
	Cg1	124.25 ± 3.64	0.37 ± 0.18	$t = 46.28$***			
	PrL	120.75 ± 3.67	0.38 ± 0.18	$t = 34.75$***			

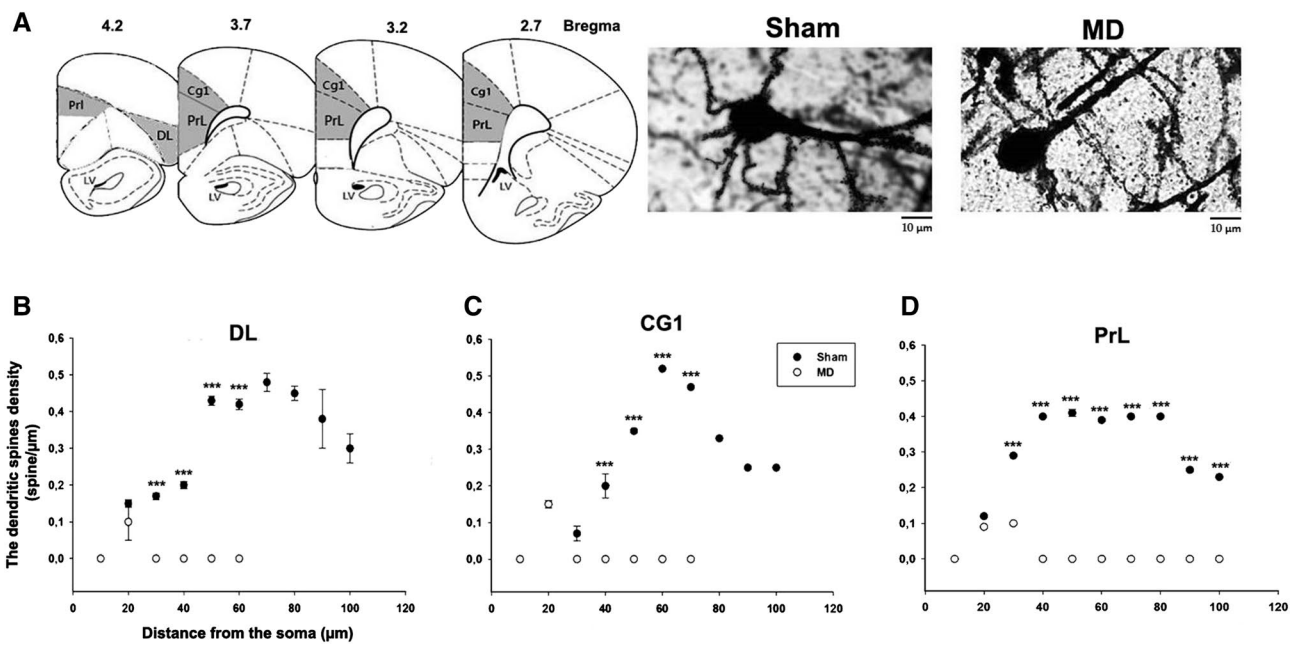*DL* dorsolateral anterior cortex, *Cg1* cingulate area1 cortex, *PrL* prelimbic cortex, *ns* non-significant

**$p < 0.01$, ***$p < 0.001$

contraction was observed in all PFC subregions of inter-est (Fig. 7a). Statistical analysis using two-way ANOVA (lesion and the region of interest as main factors) con-firmed the decrease of dendritic length of pyramidal cells of layer *V* of the PFC following MD lesion (Fig. 7b). The degree of reduction was dependent on the the subregion studied [$F(2.47) = 11.08$; $p < 0.001$]. Statistical com-parison also showed that the interaction between the two dependent factors (lesion by PFC subregion) is not sig-nificant [$F(2.47) = 2.85$, $p > 0.05$] (Fig. 7b). The post hoc analysis using the Holm-Sidak test supported these find-ings, and indicated that in all PFC subregions, the den-dritic length has significantly decreased in the MD lesion group compared to the MD sham group (DL: $t = 11.26$, $p < 0.001$; Cg1: $t = 7.91$, $p < 0.001$; PrL: $t = 9.92$, $p < 0.001$).

Immunohistochemistry

C-Fos immunolabeling in the PFC

Our results clearly showed that the early MD lesion dis-rupted neuronal activation in the PFC expressed as a decrease in the mean number of C-Fos+ neurons in MD lesion animals (Fig. 8a–c). Statistical analysis using two-way ANOVA (the lesion and the PFC subregion as independent factors) showed that the early MD lesion caused a significant decrease in the mean number of C-Fos+ neurons in the PFC [$F(1.47) = 147.00$, $p < 0.001$] (Fig. 8c). This analysis also revealed a significant inter-action between the lesion and the localization of the C-Fos+ neuron, showing that the effect of MD lesion caused a significant decrease in C-Fos expression within the PFC, but the degree of the decrease depended on the

Fig. 6 Sholl analysis showing the mean spine density vs distance from the soma. **a** Schematic drawing of coronal rat brain sections of the PFC showing the three subregions of interest (in *gray*), and representative photomicrographs of MD sham and MD lesion pyramidal neurons. **b** Mean spine density vs distance from the soma in DL. **c** Mean spine density vs distance from the soma in Cg1. **d** Mean spine density vs distance from the soma in PrL. *DL* dorsolateral anterior cortex, *Cg1* cingulate area1 cortex, *PrL* prelimbic cortex. Data presented as mean ± SEM. ***$p < 0.001$ refers to the MD sham vs MD lesion groups' comparison
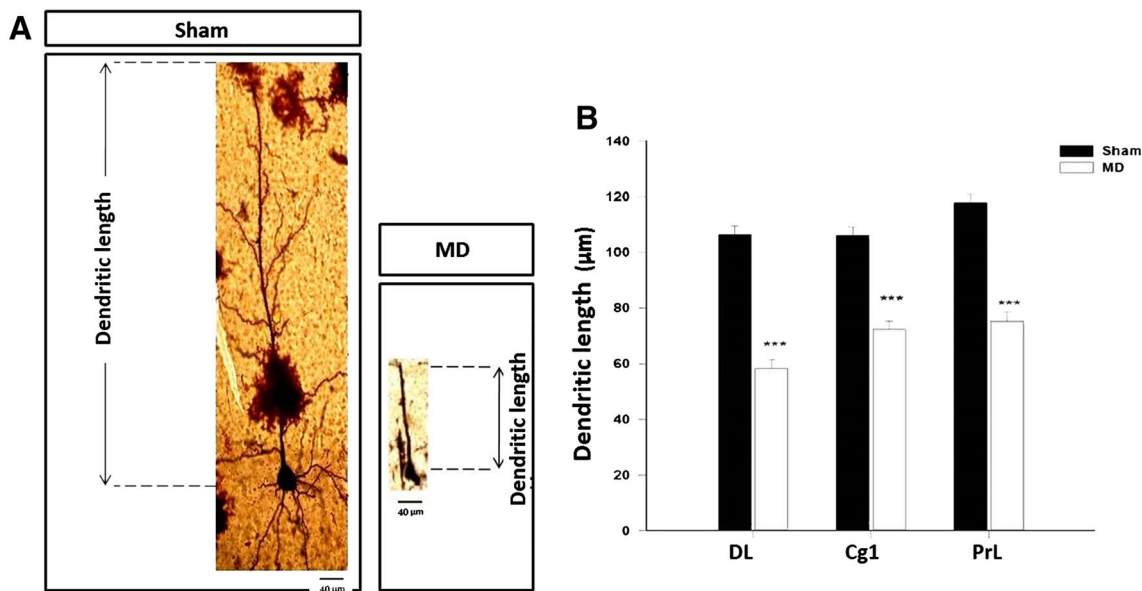

Fig. 7 Effects of MD lesion on dendritic length. **a** Photomicrographs showing a pyramidal neuron from MD sham PFC vs a pyramidal neuron of MD lesion. **b** Mean of dendritic length quantified using Sholl analysis. Data presented as mean ± SEM. ***$p < 0.001$ refers to the MD sham vs MD lesion groups' comparison

studied subregion [$F(2.47) = 29.65$, $p < 0.001$] (Fig. 8c). The *post hoc* analysis using Holm-Sidak method attested that the early MD lesion caused a significant decrease in the mean of total C-Fos+ neurons in the PFC (DL:
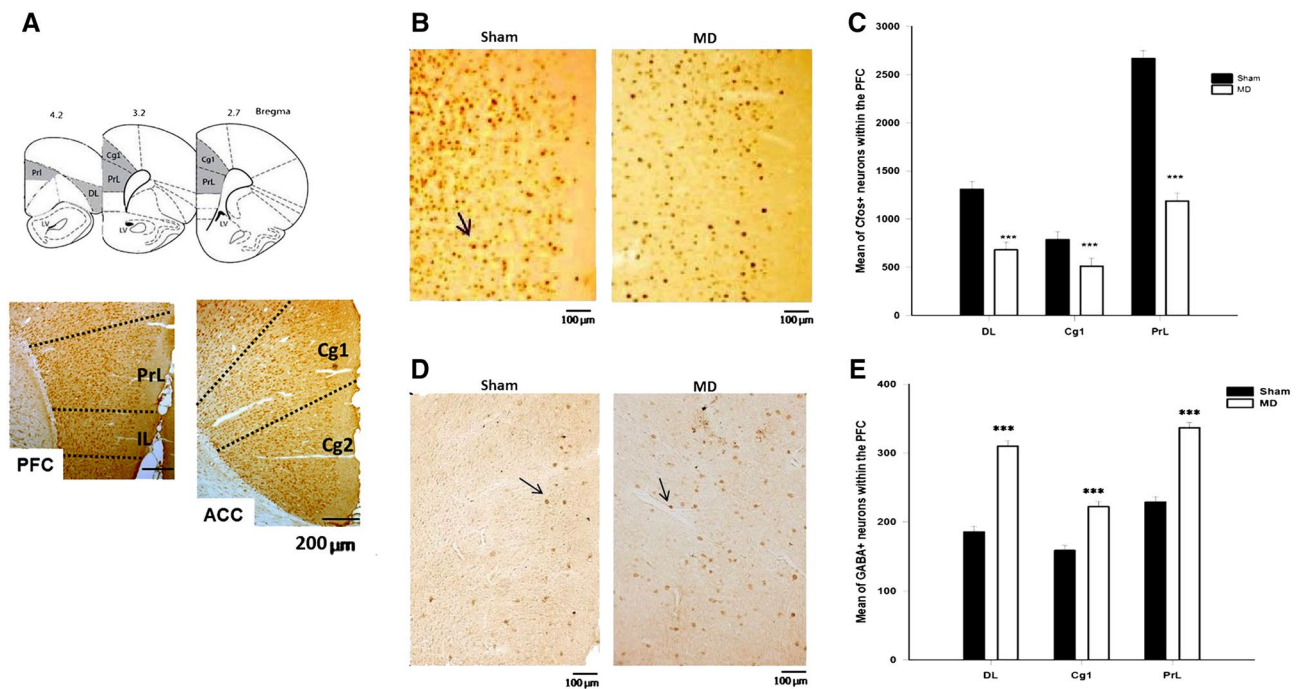
Fig. 8 C-Fos+ (*arrow* **b**–**d**) and GABA+ neurons in the PFC. **a** Schematic drawing of coronal rat brain sections of the PFC and photomicrographs of "Immunohistochemistry" showing the three subregions of interest (in *gray*). **b** Representative photomicrographs of the C-Fos+ (*arrow*) distribution in the PFC (PrL) in MD sham and MD lesion groups. **c** Mean of total number of C-Fos+ neurons within the PFC. **d**: Representative photomicrographs of the GABA+ neurons (*arrow*) within the PFC (PrL) in MD sham and MD lesion groups. **e** Mean of total number of GABA+ neurons within the PFC. Data presented as mean ± SEM. ***$p < 0.001$ refers to the MD sham vs MD lesion groups' comparison. *PFC* prefrontal cortex, *ACC* anterior cingulate cortex, *PrL* prelimbic cortex, *IL* infralimbic cortex, *Cg1* anterior cingulate cotex1, *Cg2* anterior cingulate cortex2

$t = 5.53$, $p < 0.001$; Cg1: $t = 2.44$, $p < 0.05$; PrL: $t = 13.03$, $p < 0.001$).

C-Fos-immunolabeling in the BLA

During this study, we also quantified C-Fos reactivity in the BLA in the early MD lesion model (Fig. 9a). Statistical analysis using the Mann–Whitney-U test revealed that the early MD lesion induced a significant increase of C-Fos+ neurons [$U = 0.0$, $p < 0.001$] (Fig. 9b).

GABA-immunolabeling in the PFC

Our data demonstrated that the MD lesion produced an increase of the mean number of GABA+ neurons in all PFC subregions. Statistical analysis using two-way ANOVA (with lesion and PFC subregion as main factors) revealed that the early MD lesion induced a significant increase of GABA+ neurons in all PFC subregions studied [$F(1.13) = 3729$, $p < 0.001$] (Fig. 8c, d). *Post hoc* analysis using the Holm-Sidak test confirmed a highly significant increase in the number of GABA+ neurons in all subregions of the PFC in MD lesion animals compared to MD

sham controls (DL: $t = 73.06$, $p < 0.001$, Cg1: $t = 61.25$, $p < 0.001$ and PrL: $t = 53.71$, $p < 0.001$) (Fig. 8d).

GABA-immunolabeling in the BLA

Interestingly, our results showed that early MD lesion attenuated inhibition in the BLA by reducing the number of its GABA+ cells (Fig. 9c, d). Statistical analysis using student's t-test demonstrated that the MD lesion caused a significant loss of GABA+ neurons in the BLA of the MD lesion group compared to the MD sham group [$t(\text{ddl} = 14) = 64.15$, $p < 0.001$]. Post-hoc analysis using the Holm-Sidak test confirmed these differences ($t = 64.15$, $p < 0.001$) (Fig. 9d).

Discussion

Our experiments have provided several main findings to support our hypothesis that early damage to the MD results in behavioral, functional, morphological, and structural deficits. Following early MD lesion at P4, rats tested in adulthood displayed more anxiety-like behaviors in the elevated plus maze and a disrupted recognition memory when
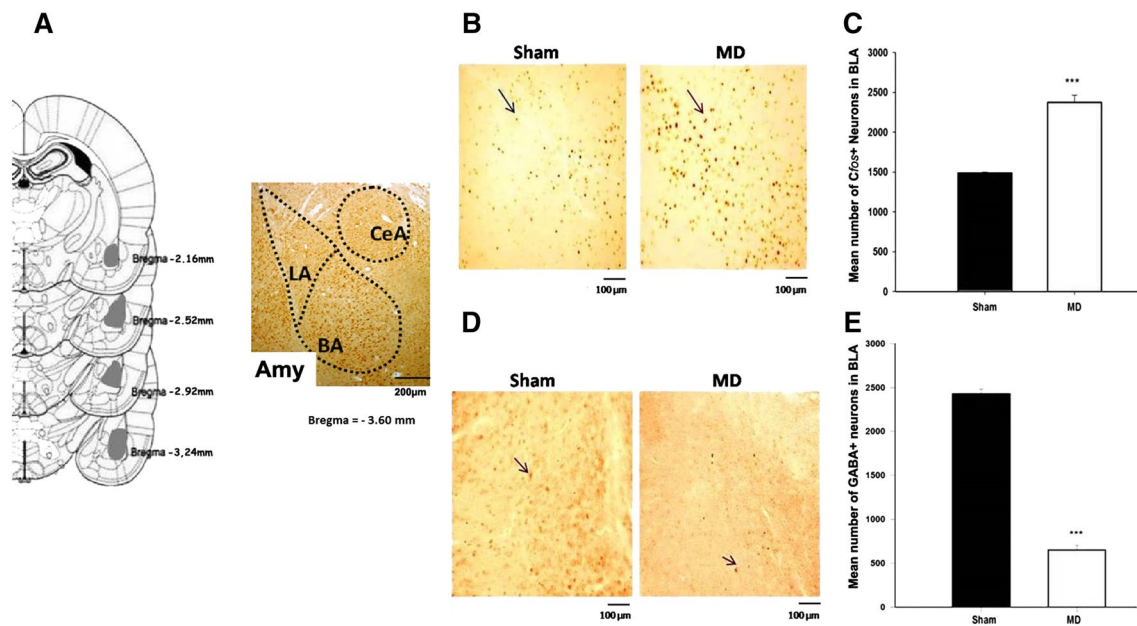
Fig. 9 C-Fos+ and GABA+ (*arrows* **b–d**) neurons in the basolateral nucleus of the amygdala (BLA). **a** Schematic representation of frontal sections of rat BLA, the *gray zone* represents BLA localization, with a photomicrograph of brain section showing the different nuclei of the amygdala. **b** Representative photomicrographs of the C-Fos+ neurons (*arrows*) distribution in the BLA in MD sham and MD lesion groups. **c** Mean (±SEM) of total number of C-Fos+ neurons within the BLA. **d** Representative photomicrographs of the GABA+ neurons (*arrows*) within the BLA in MD sham and MD lesion groups. **e** Mean of total number of GABA+ neurons within the PFC. Data presented as mean ± SEM. ***$p < 0.001$ refers to the MD sham vs MD lesion groups' comparison. *LA* Lateral amygdala, *BA* Basal amygdala, *CeA* Central nucleus of the amygdala, *Amy* Amygdala

tested in the novel object recognition paradigm. These behavioral alterations could be attributed in part to the MD lesion itself and also to the morphological and structural changes in the PFC and BLA, reflecting a disruption of the MD-PFC-BLA circuitry. The morphological effects of the lesion on the development of the PFC indicate a significant decrease in basal and apical dendritic branching in the Cg1, DL, and PrL subregions of the PFC. We also found a reduction of the dendritic length coupled with an important loss of spine density, in both primary and secondary dendrites of pyramidal neurons. Adult MD lesion rats compared to MD sham rats exhibited a significant increase in GABAergic neurons in PFC subregions, whereas in the BLA, the density of the same neuronal population was significantly decreased.

The lesion procedure and timing. MD lesions were performed on P4 using electrolytic heating. This procedure damages cell bodies as well as axons passing through the lesion site. Although our lesions were confined to the MD, additional non-specific damage to fibers of passage might have occurred. Therefore, we cannot exclude that the morphological, structural, functional, and behavioral alterations in the MD lesion rats may in part result from dysfunction in cortical–thalamo–cortical projections associated with the MD as well as cortical projections of the MD to the amygdala. The early postnatal period (from P1 to P10) in the rat brain is characterized by dramatic changes contributing to synaptic formation, growth, regression, and stabilization of connections (Cotman and Nieto-Sampedro 1984). In the early postnatal weeks, the PFC matures both morphologically and functionally. Thus, at P7, all cytoarchitectural layers of the PFC become distinguishable, but are still very immature (Van Eden and Uylings 1985). Around P14, the cortical layers in the orbital PFC subarea reach their adult proportional width, whereas in the medial PFC the cytoarchitecture of the PFC is developing up to P18 and the cortical layers attain their adult proportional width around P24 (Van Eden and Uylings 1985). As previously mentioned, the MD lesion was conducted on day P4, which coincides within the time window when afferent and efferent connections are forming between the MD and PFC (Van Eden 1986). In addition, during this same critical period of brain maturation (P4-P24), the distribution of projection cells from the PFC into the BLA is reorganized (Bouwmeester et al. 2002). McDonald (1998) described all currently known projections from cortical areas (PrL and the Cg1) to the amygdala (BLA and CeA) in the rat, cat, and monkey. Also, retrograde labeling studies with injections into the BLA resulted in neuronal labeling in layers III and V of the DL and PrL (Cassell et al. 1989; Hurley et al. 1991).

Behavioral phenotype. Anxiety-like behavior. MD lesions at postnatal P4 resulted in increased anxiety-like behavior in adulthood as seen in the elevated plus maze test. Similar results have been reported in our previous study using the same procedure (Ouhaz et al. 2015), and in mice with MD lesions done during in adulthood (Bishop et al. 2004; Chauveau et al. 2005), suggesting that the increase in anxiety-like behavior is not necessarily developmentally driven. Notably, the elevated plus maze test involves a motivational conflict between the rats' innate tendency to explore a novel environment and their innate fear of open spaces (Phifer and Terry 1986). Our MD lesion rats are more likely to explore the closed arms of the elevated plus maze compared to animals from the MD sham group. Anxiety is not only associated with an increased responsiveness to potential threats, but also with heightened distractibility and poor concentration (Lacroix et al. 1998).

Neuroimaging evidence demonstrates a link between anxiety-like behaviors and the medial PFC in humans (Bishop et al. 2004), although there are mixed results on measures of anxiety-like behavior in rat models after medial PFC lesions (Lacroix et al. 1998; Li et al. 2010). Consequently, our novel evidence of changes in levels of anxiety after early onset damage to the MD suggests that the interactions between the MD and PFC are important in anxiety-like behaviors. Taking into account the key role of the amygdala in the detection and identification of salient stimuli related to anxiety, it is still unclear to what extent amygdala nuclei are involved in the reaction to the height and open spaces of the elevated plus maze. The study of Moreira et al. (2007) showing that the BLA is involved in stimulus detection and evaluation of threatening stimuli, leading to the passive avoidance of novel, elevated, and open platforms of the elevated plus maze (File et al. 1988; Pesold and Treit 1995), is relevant to our findings. A recent study by Prager et al. (2014) provided evidence that anxiety disorders caused by nerve agent exposure are probably due to reduced GABAergic inhibition in the BLA and the increases in spontaneous excitatory activity. Interestingly, our results showed an increase of the number of GABAergic neurons within the PFC as well as a dramatic reduction in GABAergic interneurons in the BLA suggesting that early damage to the MD disrupts the capability of inhibitory inputs to regulate excitatory neurons in the BLA and causes a significant increase in glutamatergic activity. This may promote hyperactivity in the BLA network and ultimately result in the development of anxiety (Davis et al. 1994; Villarreal and King 2001; LeDoux 2003; Rauch et al. 2006; Etkin and Wager 2007).

Recognition memory. Our results highlight for the first time that early postnatal MD lesions in rats reduce the performance of the animals during the spontaneous object recognition test. The novel object recognition test takes advantage of the animal's tendency to approach and explore novelty. These results are comparable to those obtained in primates using a different procedure where the novel object is associated with a reward. Hence, MD lesions (magnocellular plus parvocellular divisions) in monkey that spared the anterior thalamic nuclei delayed reacquisition in the delayed non-matching-to-sample task (Zola-Morgan and Squire 1985). Furthermore, aspiration lesions restricted to the medial part (magnocellular) of the medial dorsal thalamic nucleus (Parker et al. 1997) also revealed a mild deficit on trial-unique delayed matching-to-sample. Finally, recording studies have found units in the medial dorsal and midline thalamic nuclei that reduce their firing rates with repetition of the same visual stimulus, though the proportions of such units were small (Fahy et al. 1993).

The results in rats appear to be less consistent. Several studies suggest that the major effect of MD lesions is not on object recognition per se, but rather on other aspects of task acquisition and performance such as sensitivity to the reinforcement contingency (McAlonan et al. 1993; Mitchell et al. 2007). Likewise, Mitchell and Dalrymple-Alford (2005) found no evidence that MD lesions disrupted spontaneous object recognition, though their rats were significantly impaired in performing recency discrimination. Thus, lesions of the MD in rats can disrupt tests of object recognition, but there is little evidence for a specific loss of recognition memory. More consistent deficits have been found for object recency, and this may reflect the close functional link between the MD and the PFC (Barker et al. 2007; Hunt and Aggleton 1998). Interestingly, crossed unilateral lesions of the MD and mPFC have demonstrated how the interplay of communication within and between MD-mPFC networks is clearly critical for associative or recency recognition memory (Cross et al. 2012). In light of all these findings concerning the implication of MD in single item recognition, our results suggest that the deficit reported in our MD lesion animals is produced by the early onset of MD damage and the disruption of MD-PFC connection during this critical phase of brain maturation.

The PFC is also critical for recognition memory and the delayed non-matching-to-sample task based on lesion studies using large aspiration of medial prefrontal cortex in rats (Kolb et al. 1994). Moreover, lesions centered on the more ventral medial prefrontal cortex (including the PrL cortex) were found to significantly impair recognition memory tasks even at short delays (Kesner et al. 1996; Ragozzino et al. 2002).

Effects of early MD lesions on spine density and dendritic morphology. The current study further quantified the effects of postnatal lesion of MD inputs on the growth and differentiation patterns of the basal and apical dendritic fields of layer V pyramidal neurons in the rat PFC. When compared to MD sham rats, MD lesion rats showed

a marked reduction of the basal dendritic field accompanied by a decrease in the number of dendritic bifurcations and a significant reduction in the length of dendritic arbors, as well as a considerable reduction in spine densities. These observations are consistent with a preliminary report on neuronal morphology of PFC neurons after early MD lesions using a similar methodology (Marmolejo et al. 2013). It should be pointed out that, in our case, the lesion size is larger and dendritic alterations are more severe (spineless pyramidal neurons) than findings reported by Marmolejo et al. (2013; 20% of the MD total volume), suggesting that the scale of changes in the PFC could be related to the extent of the lesion.

A large part of dendritic development occurs postnatally in rodents and is related to the degree of connectivity (McAllister 2000). Thalamic afferents likely participate in the cortical development and, more specifically, in the activity-dependent process of dendritic pruning (Wise et al. 1979; Van Ooyen et al. 1995; Van Pelt et al. 1996). In fact, PFC pyramidal neurons receive direct excitatory projections from the MD suggesting that loss of excitatory afferents during development may participate in this process of dendritic development and maturation. Furthermore, deafferentation causes many changes in the target regions, leading to loss of dendrites (Berry 1974).

The afferent inputs from the MD to the PFC are primarily excitatory; they arrive in the developing cortex and enter the subplate prior to the birth of their primary target cell layer (Berry 1974; Kuroda et al. 1995; Negyessy et al. 1998; Gabbot et al. 2003; Flores et al. 2005). In dysgranular cortices such as the Cg1, Prl, and DL, both layers II–III and layer V are the potential targets for thalamic afferents (Kuroda et al. 1995, 1998). Excitatory projections from the thalamus to the cortex synapse primarily on layer III and layer V apical dendrites and thin basal dendrites, possibly distal segments of the basal dendrites (Kuroda et al. 1995, 1998).

In addition to thalamic afferents (the excitatory drive), GABAergic cells play a crucial role in pyramidal cell maturation (Callaway et al. 1995; Gillessen and Alzheimer 1997). This neuronal population can deactivate dendritic voltage-sensitive channels and may prime dendrites resulting in hyperpolarization of pyramidal cells (Callaway et al. 1995; Gillessen and Alzheimer 1997), thus playing a role in controlling neuronal excitability. The GABAergic alterations reported in our study may thus contribute to the under-development of the dendritic field of PFC pyramidal neurons following early MD lesion.

Effects of early MD lesions on neuronal activation. Following behavioral testing, neuronal activation of the DL, Cg1, and PrL subregions of the PFC and the BLA was assessed by induction of the immediate gene C-Fos. Our results clearly demonstrated that early MD lesions lead to a decrease in the number of C-Fos positive neurons in all PFC subregions, whereas in the BLA complex C-Fos immunoreactive cells significantly increased in number. It has been suggested that C-Fos immunoreactivity reflects an increased neuronal discharge (Sheng and Greenberg 1990), and is expressed under basal conditions, although it is often used as a neuronal marker for responses to acute or chronic stimuli and for behavioral responses (For review see Herrera and Robertson 1996). Interestingly, the examination of the direct relationship between Fos expression and electrophysiological activity revealed that Fos expression correlates with synaptic activity levels rather than action potentials (Labiner et al. 1993; Sgambato et al. 1997). Overall, these studies support the idea that persistent and strong synaptic activity leads to Fos expression (Curran and Morgan 1986; Xing et al. 1996; Cohen and Greenberg 2008), making it an ideal parameter for our experimental design. Interestingly, the assessment of basal Fos immunoreactivity has been previously used to evaluate the long-term effects of adult brain lesions (Mena-Segovia 2004), neonatal lesions (for review see Tseng et al. 2009) or following neonatal hypoxiaischemia (Souza et al. 2014).

Effects of early MD lesions on inhibitory neurotransmission in the PFC. In the present study, we also investigated whether GABAergic interneurons in the prefrontal cortex are sensitive to the early lesion of the MD. Our results suggest that MD lesion created a synaptic reorganization by increasing the total number of GABAergic neurons in all PFC subregions. These findings do not support our initial hypothesis of a compensatory down-regulation of inhibition in the PFC in response to the reduction in excitatory inputs from the MD. The study by Volk and Lewis (2003) showed that when performed in adulthood, MD lesions had no effect on the expression of GAD67 mRNA (a synthesizing enzyme for GABA). This points to the importance of the time window when the MD lesion was performed. An interesting study using an animal model of early traumatized gerbils revealed that epigenetic disturbances during development can cause an increase of GABAergic fibers in lamina I/II of the mPFC of adult animals, further supporting the high degree of plasticity of GABAergic neurons (Brummelte et al. 2007; Dawirs et al. 1993a). There are sufficient grounds supporting the assumption that after adult deafferentation, the affected pyramidal cells were able to surmount the resulting destabilization of their input–output balance by reactive structural and functional compensation (Dammasch et al. 1986; Wolff and Wagner 1983). Thus, the question was whether or not an early MD lesion, which results in presynaptic deafferentation, may serve as a trigger for functional changes by compensatory synaptogenesis. Our results suggest that GABAergic neurons are highly involved in the neuronal reorganization of the prefrontal cortex induced by an MD lesion, and that novel

GABAergic synapses may participate in the remodeling of the pyramidal cells' inhibitory afferent inputs (see Dawirs et al. 1993b).

Concerning the area-specific maturation of GABAergic cells, previous prenatal and early postnatal investigations have demonstrated that GABAergic cells appear in the rodent visual or somatosensory cortex as early as embryonic day E14-16 (Chronwall and Wolff 1980; Del Rio et al. 1992) and that there are no apparent changes in cell density after the third postnatal week (Chronwall and Wolff 1980). Furthermore, the calbindin positive subpopulation of GABAergic neurons appeared prenatally in the rat cortex, and increased until P8-P11, but their number seemed to decrease notably between P11-P15. Numbers reached adult levels around the end of the third postnatal week (Alcantara et al. 1993). In addition, Vincent et al. (1995) found a decrease in the GABAergic cell density between P8-P15 in the mPFC of rats. The present results might be related to developmental changes rather than a possible phenotypic shift of neurons, since our MD lesions were performed before the critical period of negative regulation (P8-P15) of GABAergic cells in the PFC.

Effects of early MD lesions on inhibitory neurotransmission in the BLA. The most striking observation in our study is that in contrast to the GABAergic remodeling pattern in the PFC, early MD lesion caused a significant loss of GABAergic neurons in the BLA. To our knowledge, there is no study revealing the effects of MD lesions on GABAergic neurons in the amygdala. The apparent discrepancy might further be due to the developmental differences of particular areas. For instance, the study by Brummelte et al. (2007) examined quantitatively the postnatal maturation of GABAergic cells and fibers in the PFC and the BLA of the Mongolian gerbil, and revealed that the maturation of the GABAergic circuit in the amygdala differs slightly from that in the PFC. A concomitant decrease in GABAergic cell density was only seen in the BLA between P14 and P20. Another reason for this could be the different targets and functions of GABAergic neurons in the cortex and the amygdala. For instance, some subpopulations of GABAergic neurons are known to build basket-like structures in the BLA, but not in the cortex (Berdel and Morys 2000). Furthermore, calbindin positive GABAergic interneurons in the cortex represent a minor subpopulation (Celio 1990) whereas they constitute almost 60% of GABAergic neurons in the BLA (McDonald and Mascagni 2001).

Taken together, there are considerable structural and functional alterations in the PFC and the BLA resulting from early MD lesion. Accordingly, the behavioral alterations reported in the current study and those from our previous report (Ouhaz et al. 2015) may possibly result from a dis-balance in MD-PFC-BLA networks. Damage to the MD during this critical period of brain maturation may lead to an imbalance of excitation and inhibition drives between the PFC and the amygdala.

As we summarized in previous sections, the development of neuronal networks and cognitive functions involves many biological processes that can take decades to complete (*e.g.*, the initial formation of the connections and circuitries, followed by activity dependent refinement of these connections). As the PFC has an extended maturation period, a sustained window of plasticity may extend the developmental time window, during which an MD lesion may affect the circuitry (Uhlhaas et al. 2013). All these changes would affect related networks, including the BLA, converging thus to manifest as a network disruption. In a more broader context, converging evidence from postmortem and electrophysiological studies of schizophrenic brains, as well as findings from animal models of the disorder suggests that schizophrenia is associated with disruption of thalamo–cortical connectivity (Altman and Bayer 1995), disruptions in dendritic morphology, and GABAergic neurotransmission in the frontal lobes (Akbarian et al. 1995; Broadbelt et al. 2002; Gonzales-Burgos and; Lewis 2008; Jones et al. 2002; Thomases et al. 2013) and an elevated amygdala activation (Kosaka et al. 2002; Rauch et al. 2010). These pathophysiological alterations may contribute to cognitive and emotional processing impairments associated with the disease.

References

Abercrombie M, Johnson ML (1946) Quantitative histology of Wallerian degeneration I. Nuclear population in rabbit sciatic nerve. J Anat Lond 80:37–50

Akbarian S, Kim JJ, Potkin SG, Hagman JO, Tafazzoli A, Bunney WE, Jones EG (1995) Gene expression for glutamic acid decarboxylase is reduced without loss of neurons in prefrontal cortex of schizophrenics. Arch Gen Psychiatry 52:258–266

Alcantara S, Ferrer I, Soriano E (1993) Postnatal development of parvalbumin and calbindin D28K immunoreactivities in the cerebral cortex of the rat. Anat Embryol (Berl.) 188: 63–73

Altman J, Bayer SA (1995) Atlas of prenatal rat brain development. CRC, Boca Raton

Armstrong E, Parker B (1986) A new Golgi method for adult human brains. J Neurosci Methods 17:247–254

Barker GRI, Bird F, Alexander V, Warburton EC (2007) Recognition memory for objects, place, and temporal order: A disconnection analysis of the role of the medial prefrontal cortex and perirhinal cortex. J Neurosci 27:2948–2957

Benes FM (1989) Myelination of cortical-hippocampal relays during late adolescence. Schizophr Bull 15:585–593

Berdel B, Morys J (2000) Expression of calbindin-D28k and parvalbumin during development of rat's basolateral amygdaloid complex. Int J Dev Neurosci 18:501–513

Berendse HW, Galis de Graaf Y, Groenewegen HJ (1992) Topographical organization and relationship with ventral striatal compartments of prefrontal corticostriatal projections in the rat. J Comp Neurol 316:314–347

Berry M (1974) Development of the cerebral neocortex of the rat; in Gottlieb G (ed): Aspects of Neurogenesis. Academic Press, New York, 2:7–67

Bishop S, Duncan J, Brett M, Lawrence AD (2004) Prefrontal cortical function and anxiety: controlling attention to threat-related stimuli. Nat Neurosci 7:184–188

Bouwmeester H, Wolterink G, van Ree JM (2002) Neonatal development of projections from the basolateral amygdala to prefrontal, striatal, and thalamic structures in the rat. J Comp Neurol 442:239–249

Broadbelt K, Byne WB, Jones LB (2002) Evidence for a decrease in primary and secondary basilar dendrites on pyramidal cells in area 32 of schizophrenic prefrontal cortex. Schizophr Res 58:75–81

Brummelte S, Neddens J, Teuchert-Noodt G (2007) Alteration in the GABAergic network of the prefrontal cortex in a potential animal model of psychosis. J Neural Transm 114(5):539–547

Callaway JC, Lasser-Ross N, Ross WN (1995) IPSPs strongly inhibit climbing fiber-activated [Ca 2+]i increases in the dendrites of cerebellar Purkinje neurons. J Neurosci 15:2777–2787

Cassell MD, Chittick CA, Siegel MA, Wright DJ (1989) Collateralization of the amygdaloid projections of the rat prelimbic and infralimbic cortices. J Comp Neurol 279:235–248

Celio MR (1990) Calbindin D-28k and parvalbumin in the rat nervous system. Neuroscience 35:375–475

Chauveau F, Celerier A, Ognard R, Pierard C, Beracochea D (2005) Effects of ibotenic acid lesions of the mediodorsal thalamus on memory: relationship with emotional processes in mice. Behav Brain Res 156:215–223

Chiba T, Kayahara T, Nakano K (2001) Efferent projections of infralimbic and prelimbic areas of the medial prefrontal cortex in the Japanese monkey, Macaca fuscata. Brain Res 888:83–101

Chronwall B, Wolff JR (1980) Prenatal and postnatal development of GABA accumulating cells in the occipital neocortex of rat. J Comp Neurol 190:187–208

Cohen S, Greenberg ME (2008) Communication between the synapse and the nucleus in neuronal development, plasticity, and disease. Annu. Rev Cell. Dev Biol 24:183–209

Cotman CW, Nieto-Sampedro M (1984) Cell biology of synaptic plasticity. Science 225:1287–1294

Cross L, Brown MW, Aggleton JP, Warburton EC (2012) The medial dorsal thalamic nucleus and the medial prefrontal cortex of the rat function together to support associative recognition and recency but not item recognition. Learn Mem 20:41–50

Curran T, Morgan JI (1986) Barium modulates c-fos expression and post-translational modification. Proc Natl Acad Sci USA 83:8521–8524

Dammasch IE, Wagner GP, Wolff JR (1986) Self-stabilization of neuronal networks. I. The compensation algorithm for synaptogenesis. Biol Cybern 54(4–5):211–222

Davis M, Rainnie D, Cassell M (1994) Neurotransmission in the rat amygdala related to fear and anxiety. Trends Neurosci 17:208–214

Dawirs RR, Teuchert-Noodt G, Czaniera R (1993a) Maturation of the dopamine innervation during postnatal development of the prefrontal cortex in gerbils (Meriones unguiculatus). A quantitative immunocytochemical study. J Hirnforsch 34:281–290

Dawirs RR, Teuchert-Noodt G, Molthagen M (1993b) Indication of methamphetamine-induced reactive synaptogenesis in the prefrontal cortex of gerbils Meriones unguiculatus. Eur J Pharmacol 421:89–97

Del Rio JA, Soriano E, Ferrer I (1992) Development of GABA-immunoreactivity in the neocortex of the mouse. J Comp Neurol 326:501–526

Ennaceur A, Aggleton JP (1994) Spontaneous recognition of object configurations in rats: effects of fornix lesions. Exp Brain Res 100(1):85–92

Etkin A, Wager TD (2007) Functional neuroimaging of anxiety: a meta-analysis of emotional processing in PTSD, social anxiety disorder, and specific phobia. Am J Psychiatry 164:1476–1488

Fahy FL, Riches IP, Brown MW (1993) Neuronal signals of importance to the performance of visual recognition memory tasks: Evidence from recordings of single neurons in the medial thalamus of primates. Progr Brain Res 95:401–416

File SE, Gonzalez LE, Gallant R (1998) Role of the basolateral nucleus of the amygdala in the formation of a phobia. Neuropsychopharmacology 19:397–405

Flores G, Alquicer G, Silva-Gomez AB, Zaldivar G, Stewart J, Quirion R, Srivastava LK (2005) Alterations in dendritic morphology of prefrontal cortical and nucleus accumbens neurons in post-pubertal rats after neonatal excitotoxic lesions of the ventral hippocampus. Neuroscience 133:463–470

Floresco SB, Braaksma DN, Phillips AG (1999) Thalamic–cortical–striatal circuitry subserves working memory during delayed responding on a radial arm maze. J Neurosci 19:11061–11071

Gabbott PL, Warner TA, Jays PR, Bacon SJ (2003) Areal and synaptic interconnectivity of prelimbic (area 32), infralimbic (area 25) and insular cortices in the rat. Brain Res 993:59–71

Garey LJ, Ong WY, Patel TS et al (1998) Reduced dendritic spine density on cerebral cortical pyramidal neurons in schizophrenia. J Neurol Neurosurg Psychiatry 65:446–453

Ghashghaei HT, Barbas H (2002) Pathways for emotion: interactions of prefrontal and anterior temporal pathways in the amygdala of the rhesus monkey. Neuroscience 115(1261):1279

Giguere M, Goldman-Rakic PS (1988) Mediodorsal nucleus: areal, laminar and tangential distribution of afferents and efferents in the frontal lobe of rhesus monkeys. J Comp Neurol 277:195–213

Gillessen T, Alzheimer C (1997) Amplification of EPSPs by low Ni 2 + and amiloride-sensitive Ca 2+ channels in apical dendrites of rat CA1 pyramidal neurons. J Neurosci 77:1639–1643

Glantz LA, Lewis DA (2000) Decreased dendritic spine density on prefrontal cortical pyramidal neurons in schizophrenia. Arch Gen Psychiatry 57:65–67

Goldman-Rakic PS, Porrino LJ (1985) The primate mediodorsal (MD) nucleus and its projection to the frontal lobe. J Comp Neurol 242:535–560

Gonzalez-Burgos G, Lewis DA (2008) NMDA receptor hypofunction, parvalbumin-positive neurons, and cortical gamma oscillations in schizophrenia. Schizophr Bull 38:950–957

Groenewegen HJ (1988) Organization of the afferent connections of the mediodorsal thalamic nucleus in the rat, related to the mediodorsal-prefrontal topography. Neuroscience 24:379–431

Guldin WO, Pritzel M, Markowitsch HJ (1981) Prefrontal cortex of the mouse defined as cortical projection area of the thalamic mediodorsal nucleus. Brain Behav Evol 19:93–107

Handley SL, McBlane JW (1993) An assessment of the elevated plus-maze for studying anxiety and anxiety-modulating drugs. J Pharmacol Toxicol Methods 29:129–138

Handley SL, Mithani S (1984) Effects of alpha-adrenoceptor agonists and antagonists in a maze-exploration model of 'fear'-motivated behavior. Naunyn Schmiedebergs Arch Pharmacol 327:1–5

Herrera DG, Robertson HA (1996) Activation of c-fos in the brain. Prog Neurobiol 50:83–107

Howard MW, Rizzuto DS, Caplan JB, Madsen JR, Lisman J, Aschenbrenner-Scheibe R, Schulze-Bonhage A, Kahana MJ (2003) Gamma oscillations correlate with working memory load in humans. Cereb Cortex 13:1369–1374

Hunt PR, Aggleton JP (1998) Neurotoxic lesions of the dorsomedial thalamus impair the acquisition but not the performance of delayed matching to place by rats: A deficit in shifting response rules. J Neurosci 18:10045–10052

Hurley KM, Herbert H, Moga MM, Saper CB (1991) Efferent projections of the infralimbic cortex of the rat. J Comp Neurol 308:249–276

Isseroff A, Rosvold HE, Galkin TW, Goldman-Rakic PS (1982) Spatial memory impairments following damage to the mediodorsal nucleus of the thalamus in rhesus monkeys. Brain Res 232:97–113

Jones L, Johnson N, Byne W (2002) Alterations in MAP2 staining in area 9 and 32 of schizophrenic prefrontal cortex. Psychiatry Res 114:137–148

Kesner RP, Hunt ME, Williams JM, Long JM (1996) Prefrontal cortex and working memory for spatial response, spatial location, and visual object information in the rat. Cereb Cortex 6:311–318

Kolb B, Buhrmann K, McDonald R, Sutherland RJ (1994) Dissociation of the medial prefrontal, posterior parietal, and posterior temporal cortex for spatial navigation and recognition memory in the rat. Cereb Cortex 4:664–680

Kosaka H, Omori M, Murata T, Iidaka T, Yamada H, Okada T, Takahashi T, Sadato N, Itoh H, Yonekura Y, Wada Y (2002) Differential amygdala response during facial recognition in patients with schizophrenia: an fMRI study. Schizophr Res 57:87–95

Krettek JE, Price JL (1977) The cortical projections of the mediodorsal nucleus and adjacent thalamic nuclei in the rat. J Comp Neurol 171:157–192

Kuroda M, Murakami K, Kishi K, Price JL (1995) Thalamocortical synapses between axons from the mediodorsal thalamic nucleus and pyramidal cells in the prelimbic cortex of the rat. J Comp Neurol 356:143–151

Kuroda M, Yokofujita J, Murakami K (1998) An ultrastructural study of the neural circuit between the prefrontal cortex and the mediodorsal nucleus of the thalamus. Prog Neurobiol 54:417–458

Labiner DM, Butler LS, Cao Z, Hosford DA, Shin C, McNamara JO (1993) Induction of c-fos mRNA by kindled seizures: complex relationship with neuronal burst firing. J Neurosci 13:744–751

Lacroix L, Broersen LM, Weiner I, Feldon J (1998) The effects of excitotoxic lesion of the medial prefrontal cortex on latent inhibition, prepulse inhibition, food hoarding, elevated plus maze, active avoidance and locomotor activity in the rat. Neuroscience 84:431–442

Lapiz-Bluhm MD, Bondi CO, Doyen J, Rodriguez GA, Bedard-Arana T, Morilak DA (2008) Behavioral assays to model cognitive and affective dimensions of depression and anxiety in rats. J Neuroendocrinol 20:1115–1137

LeDoux J (2003) The emotional brain, fear, and the amygdala. Cell Mol Neurobiol 23:727–738

Leonard CM (1969) The prefrontal cortex of the rat. I. Cortical projection of the mediodorsal nucleus. II. Efferent connections. Brain Res 12(2):321–343

Li CR, Huang GB, Sui ZY, Han EH, Chung YC (2010) Effects of 6-hydroxydopamine lesioning of the medial prefrontal cortex on social interactions in adolescent and adult rats. Brain Res 1346:183–189

Lipska BK, Weinberger DR (1993) Delayed effects of neonatal hippocampal damage on haloperidol induced catalepsy and apomorphine-induced stereotypic behaviours in the rat. Dev Brain Res 75:213–222

Maaswinkel H, Gispen WH, Spruijt BM (1996) Effects of an electrolytic lesion of the prelimbic area on anxiety-related and cognitive tasks in the rat. Behav Brain Res 79:51–59

Marmolejo N, Paez J, Levitt JB, Jones LB (2012) Early postnatal lesion of the medial dorsal nucleus leads to loss of dendrites and spines in adult prefrontal cortex. Dev Neurosci 34(6):463–476

Marmolejo N, Paez J, Levitt JB, Jones LB (2013) Early postnatal lesion of the medialdorsal nucleus leads to loss of dendrites and spines in adult prefrontal cortex. Dev Neurosci 34:463–476

McAllister AK (2000) Cellular and molecular mechanisms of dendrite growth. Cereb Cortex 10(10):963–973

McAlonan GM, Robbins TW, Everitt BJ (1993) Effects of medial dorsal thalamic and ventral pallidal lesions on the acquisition of a conditioned place preference: further evidence for the involvement of the ventral striatopallidal system in reward-related processes. Neuroscience 52:605–620

McDonald AJ (1991) Organization of amygdaloid projections to the prefrontal cortex and associated striatum in the rat. Neuroscience 44:1–14

McDonald AJ (1998) Cortical pathways to the mammalian amygdala. Progr Neurobiol 55:257–332

McDonald AJ, Mascagni F (2001) Colocalization of calcium-binding proteins and GABA in neurons of the rat basolateral amygdala. Neuroscience 105:681–693

McDonald AJ, Mascagni F, Guo L (1996) Projections of the medial and lateral prefrontal cortices to the amygdala: a Phaseolus vulgaris leucoagglutinin study in the rat. Neuroscience 71:55–75

Mitchell AS, Dalrymple Alford JC (2005) Dissociable memory effects after medial thalamus lesions in the rat. Eur J Neurosci 22:973–985

Mitchell AS, Browning PGF, Baxter MG (2007) Neurotoxic lesions of the medial mediodorsal nucleus of the thalamus disrupt reinforcer devaluation effects in rhesus monkeys. J Neurosci 27:11289–11295

Moreira CM, Masson S, Carvalho MC, Brandao ML (2007) Exploratory behaviour of rats in the elevated plus maze is differentially sensitive to inactivation of the basolateral and central amygdaloid nuclei. Brain Res Bull 71:466–474

Negyessy L, Hámori J, Bentivoglio M (1998) Contralateral cortical projection to the mediodorsal thalamic nucleus: origin and synaptic organization in the rat. Neuroscience 84:741–753

Ottersen OP, Ben-Ari Y (1979) Afferent connections to the amygdaloid complex of the rat and cat. J Comp Neurol 187:401–424

Ouhaz Z, Ba-M'hame S, Mitchell AS, Elidrissi A, Bennis M (2015) Behavioral and cognitive changes after early postnatal lesions of the rat mediodorsal thalamus. Behav Brain Res 292:219–232

Parker A, Eacott MJ, Gaffan D (1997) The recognition memory deficit caused by mediodorsal thalamic lesion in non-human primates: A comparison with rhinal cortex lesion. Eur J Neurosci 9:2423–2431

Parnaudeau S, O'Neill PK, Bolkan SS, Ward RD, Abbas AI, Roth BL, Balsam PD, Gordon JA, Kellendonk C (2013) Inhibition of mediodorsal thalamus disrupts thalamofrontal connectivity and cognition. Neuron 77:1151–1162

Parnaudeau S, Taylor K, Bolkan SS, Ward RD, Balsam PD, Kellendonk C (2015) Mediodorsal thalamus hypofunction impairs flexible goal-directed behavior. Biol Psychiatry 77:445–453

Paxinos G, Watson C (2008) The rat brain: in stereotaxic coordinates, vol 6. Elsevier Academic Press, San Diego

Pesold C, Treit D (1995) The central and basolateral amygdala differentially mediate the anxiolytic effects of benzodiazepines. Brain Res 671:213–221

Phelps EA, Le Doux JE (2005) Contributions of the amygdala to emotion processing: from animal models to human behavior. Neuron 48:175–187

Phifer CB, Terry LM (1986) Use of hypothermia for general anesthesia in preweanling rodents. Physiol Behav 38:887–890

Prager EM, Pidoplichko VI, Aroniadou-Anderjaska V, Apland JP, Braga MF (2014) Pathophysiological mechanisms underlying increased anxiety after soman exposure: reduced GABAergic inhibition in the basolateral amygdala. Neurotoxicology 44:335–343

Quirk GJ, Beer JS (2006) Prefrontal involvement in the regulation of emotion: convergence of rat and human studies. Curr Opin Neurobiol 16:723–727

Ragozzino M, Detrick S, Kesner R (2002) The effects of prelimbic and infralimbic lesions on working memory for visual objects in rats. Neurobiol Learn Mem 77:29–43

Rajan I, Cline HT (1998) Glutamate receptor activity is required for normal development of tectal cell dendrites in vivo. J Neurosci 18:7836–7846

Rauch SL, Shin LM, Phelps EA (2006) Neurocircuitry models of posttraumatic stress disorder and extinction: human neuroimaging research – past, present, and future. Biol Psychiatry 60:376–382

Rauch AV, Reker M, Ohrmann P, Pedersen A, Bauer J, Dannlowski U, Harding L, Koelkebeck K, Konrad C, Kugel H, Arolt V, Heindel W, Suslow T (2010) Increased amygdala activation during automatic processing of facial emotion in schizophrenia. Psychiatry Res 182:200–206

Rios O, Villalobos J (2004) Postnatal development of the afferent projections from the dorsomedial thalamic nucleus to the frontal cortex in mice. Dev Brain Res 150(1):47–50

Room P, Russchen FT, Groenewegen HJ, Lohman AH (1985) Efferent connections of the prelimbic (area 32) and the infralimbic (area 25) cortices: An anterograde tracing study in the cat. J Comp Neurol 242:40–55

Rose JE, Woolsey CN (1948) The orbitofrontal cortex and its connections with the mediodorsal nucleus in rabbit, sheep and cat. Res Publ Assoc Res Nerv Ment Dis 27(1):210–232

Sah P, Faber ESL, Lopez de Armentia M, Power J (2003) The amygdaloid complex: anatomy and physiology. Physiol Rev 83(3):803–834

Sesack SR, Deutch AY, Roth RH, Bunney BS (1989) Topographical organization of the efferent projections of the medial prefrontal cortex in the rat: An anterograde tract-tracing study with Phaseolus vulgaris leucoagglutinin. J Comp Neurol 290:213–242

Sgambato V et al (1997) Effect of electrical stimulation of the cerebral cortex on the expression of the Fos protein in the basal ganglia. Neuroscience 81:93–112

Sheng M, Greenberg ME (1990) The regulation and function of c-fos and other immediate early genes in the nervous system. Neuron 4:477–485

Shinonaga Y, Takada M, Mizuno N (1994) Topographic organization of collateral projections from the basolateral amygdaloid nucleus to both the prefrontal cortex and nucleus accumbens in the rat. Neuroscience 58:389–397

Sholl DA (1953) Dendritic organization in the neurons of the visual and motor cortices of the cat. J Anat 87(4):387–406

Silva-Gomez AB, Rojas D, Juarez I, Flores G (2003) Decreased dendritic spine density on prefrontal cortical and hippocampal pyramidal neurons in postweaning social isolation rats. Brain Res 983:128–136

Souza A, Dussan-Sarria JA, Medeiros LF, Souza AC, Oliveira C, Scarabelot VL, Adachi LN, Winkelmann-Duarte EC, Philippi-Martins BB, Netto CA, Caumo W, Torres ILS (2014) Neonatal hypoxic–ischemic encephalopathy reduces c-Fos activation in the rat hippocampus: evidence of a long-lasting effect. Int J Dev Neurosci 38:213–222

Su HS, Bentivoglio M (1990) Thalamic midline cell populations projecting to the nucleus accumbens, amygdala and hippocampus in the rat. J Comp Neurol 297:582–593

Thompson M, Weickert CS, Wyatt E, Webster MJ (2009) Decreased glutamic acid decarboxylase67 mRNA expression in multiple brain areas of patients with schizophrenia and mood disorders. J Psychiatr Res 43(11):970–977

Thomases DR, Cass DK, Tseng KY (2013) Periadolescent exposure to the NMDA receptor antagonist MK-801 impairs the functional maturation of local GABAergic circuits in the adult prefrontal cortex. J Neurosci 33:26–34

Tseng KY, Chambers RA, Lipska BK (2009) The neonatal ventral hippocampal lesion as a heuristic neurodevelopmental model of schizophrenia. Behav Brain Res 204:295–305

Uhlhaas PJ, Roux F, Singer W (2013) Thalamocortical synchronization and cognition: implications for schizophrenia? Neuron 77(6):997–999

Uylings HB, Groenewegen HJ, Kolb B (2003) Do rats have a prefrontal cortex? Behav BrainRes 146:3–17

Van Eden CG (1986) Development of connections between the mediodorsal nucleus of the thalamus and the prefrontal cortex in the rat. J Comp Neurol 244:349–359

Van Eden CG, Uylings HB (1985) Postnatal volumetric development of the prefrontal cortex in the rat. J Comp Neurol 241:268–274

Van Ooyen A, van Pelt J, Corner MA (1995) Implication of activity-dependent neurite outgrowth for neuronal morphology and network development. J Theor Biol 172:63–82

Van Pelt J, van Ooyen A, Corner MA (1996) Growth cone dynamics and activity-dependent processes in neuronal network development. Prog Brain Res 108:333–346

Vertes RP (2004) Differential projections of the infralimbic and prelimbic cortex in the rat. Synapse 51(1):32–58

Villarreal G, King CY (2001) Brain imaging in posttraumatic stress disorder. Semin Clin Neuropsychiatry 6:131–45

Vincent SL, Pabreza L, Benes FM (1995) Postnatal maturation of GABA immunoreactive neurons of rat medial prefrontal cortex. J Comp Neurol 355:81–92

Volk DW, Lewis DA (2003) Effects of a mediodorsal thalamus lesion on prefrontal inhibitory circuitry: implications for schizophrenia. Biol Psychiatry 53:385–389

Volk DW, Austin MC, Pierri JN, Sampson AR, Lewis DA (2000) Decreased glutamic acid decarboxylase67 messenger RNA expression in a subset of prefrontal cortical gammaaminobutyric acid neurons in subjects with schizophrenia. Arch Gen Psychiatry 57:237–245

Wise SP, Fleshman JW, Jones EG (1979) Maturation of pyramidal cell form in relation to developing afferent and efferent connections of the rat somatic sensory cortex. J Neurosci 4:1275–1297

Wolff JR, Wagner GP (1983) Self organization in synaptogenesis: interaction between the formation of excitatory and inhibitory synapses. In: Basar F, Flohr H, Haken H, Mandell AJ. (eds) Synergetics in the brain. Springer, Berlin, pp 50–59

Xing J, Ginty DD, Greenberg ME (1996) Coupling of the RAS-MAPK pathway to gene activation by RSK2, a growth factor-regulated CREB kinase. Science 273:959–963

Zola-Morgan S, Squire LR (1985) Amnesia in monkeys after lesions of the mediodorsal nucleus of the thalamus. Ann Neurol 17:558–564